250 GHz Cold Tests for the LLNL CARM Experiment*

B. Kulke, M. Caplan, R. Stever
Lawrence Livermore National Laboratory
P. O. Box 808, Livermore, California 94550

Abstract

A cyclotron autoresonant maser (CARM) experiment has been designed and built for operation at 250 GHz, in conjunction with the LLNL ARC induction linac. Beam parameters are 2 MeV, 1 kA, 30 ns. The RF structures tested consist of 7 mm diam, 9-18 cm long Bragg sections. These sections are electroformed, with 50-90 μm deep, sinusoidal ripples spaced at half wavelength intervals. A shallow ripple depth is essential in separating the desired, TE_{11} resonance from neighboring resonances that are excited by mode conversion. We present code results and validating cold test data that illustrate the sensitivity of mode separation to ripple depth. We also present design calculations and calibration data at 250 GHz for a 2 m long, microwave diffraction tank.

I. INTRODUCTION

The LLNL CARM experiment was intended to demonstrate the generation of high-power millimeter waves near 250 GHz, using the 2 MeV, 1 kA, 30 ns beam at the ARC facility as an energy source. The choice of frequency was dictated by the potential application as a high-power source for current drive and disruption control in Alcator-C, an ongoing tokamak experiment. The use of Bragg reflectors in a waveguide environment is well understood,[1] although their application at 250 GHz is new, and poses some challenging fabrication problems. The Bragg reflectors can be used either as standalone resonators or as reflective terminations bracketing a smooth-walled resonator section. We used the first configuration for the CARM experiment, in an oscillator-amplifier configuration.[2] The microwave power generated was allowed to radiate into a diffraction tank; the design of this tank is discussed in the latter part of this note.

II. BRAGG SECTION DESIGN AND PERFORMANCE

A cylindrical waveguide can be made into a Bragg section by corrugating sections of wall with sinusoidal ripples that are spaced one-half wavelength apart. Minute reflections from each ripple add up in phase so that by using a large enough number of ripples, an arbitrary amount of reflection of the microwave signal may be achieved, essentially without affecting the waveguide cross section available for, e.g., electron beam passage. Increasing the ripple depth results in greater reflectivity, but also enhances mode conversion and hence must be done with caution. For the CARM experiments, the beam pipe diameter was chosen at 7 mm to allow propagation in the TE_{11} mode at ten times the waveguide cutoff, or 250 GHz. We designed, built, and fully characterized Bragg reflectors with 150 and 300 sinusoidal, 25 μm amplitude ripples. We also built a 300-ripple Bragg section with 45 μm amplitude corrugations, which was used as a standalone resonator in the oscillator-amplifier configuration. This section was not cold tested because we had damaged the necessary diagnostic equipment during earlier beam tests. The ripple period for all sections was 0.6 mm.

The Bragg sections were manufactured at LLNL. The sinusoidal ripple contour was machined into an aluminum plating mandrel to a nominal precision of 100 microinches, using a diamond tool leaving a 16-microinch surface finish. This mandrel was then copper plated and etched away to leave the sinusoidal contour. The Bragg section was then machined to the correct length and the waveguide flanges were attached. For the 45-μm ripple section, the copper plating was made sufficiently massive to allow direct machining of the flanges, thus avoiding the thermal stresses and possible distortion due to soldering.

Analytical expressions for the single-mode reflection coefficients of a Bragg section are available.[1] While these are quite useful for yielding design approximations quickly, they tend to be in error when there is significant Bragg reflection in more than one mode. A more accurate model can be had with a coupled-mode theory and simulation code developed by M. Caplan, which self-consistently considers both forward and reflected wave components of two or more coupled waveguide modes in the presence of wall discontinuities. It turns out that in order to achieve good separation in frequency between the desired, pure TE_{11} reflection region and the adjacent, undesirable TM_{11} region, it is necessary to use a large number of shallow ripples. This is illustrated in Fig. 1, which plots the theoretical, reflected power vs. frequency for a Bragg section with varying ripple number and depth. Figure 2 shows our cold test setup. In order to avoid trapped modes, we coupled the open Bragg section quasioptically to the detector horn, which was placed well into the far-field region. The Bragg section partly reflects the incident TE_{11} power and partly converts it into the TM_{11} mode; however, the latter has a null on axis and is not detected by the receiver, so that the converted power simply registers as more insertion loss. Figure 3 shows the measured insertion loss obtained with a 300 ripple, 25 μm section; the agreement with the theory is seen to be quite good. This result was replicated accurately with two separate, identical Bragg sections, which attests to the accuracy of the machining. Figure 4 shows similar data taken for a shorter section (150 ripples); there is an amplitude disagreement on the order of 10 dB with the theory which is not understood. We also tested the insertion loss of a smooth-pipe section terminated by a short Bragg section at each end, and obtained reasonable agreement with the three resonant peaks predicted from the theory.

*Work performed under the auspices of the U.S. Department of Energy by Lawrence Livermore National Laboratory under contract No. W-7405-ENG-48.

0-7803-0135-8/91$01.00 ©IEEE

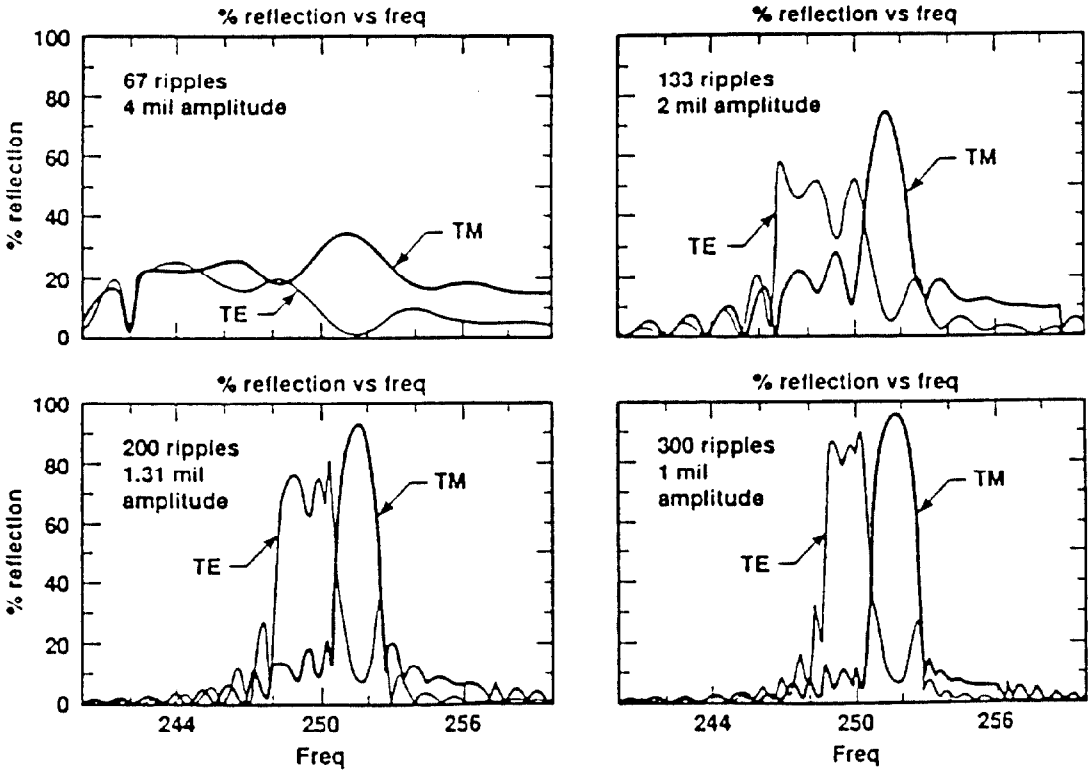

Fig. 1. Two-mode calculation of TE and TM mode reflected power, for different ripple parameters in a 7-mm-diam Bragg section. Good mode separation requires many ripples of small amplitude.

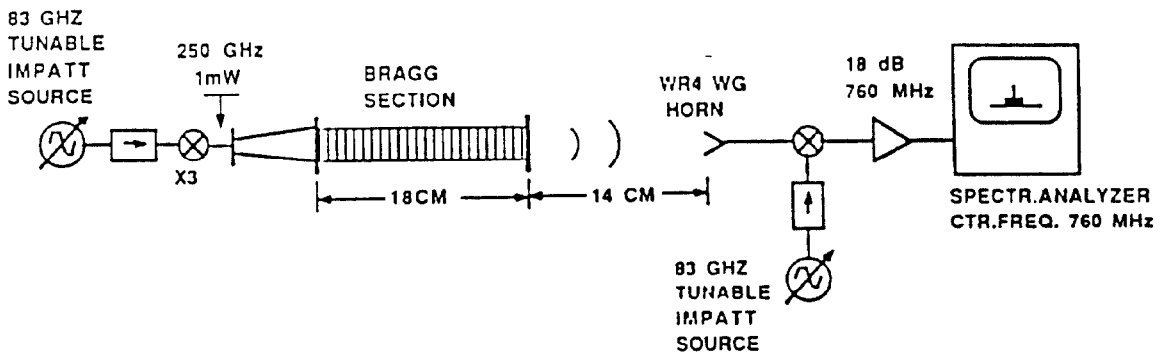

Fig. 2. Apparatus used for insertion loss measurement on Bragg sections. A substitution method was used, with a smooth pipe section as reference. Trapped modes were avoided by leaving the Bragg section open-ended.

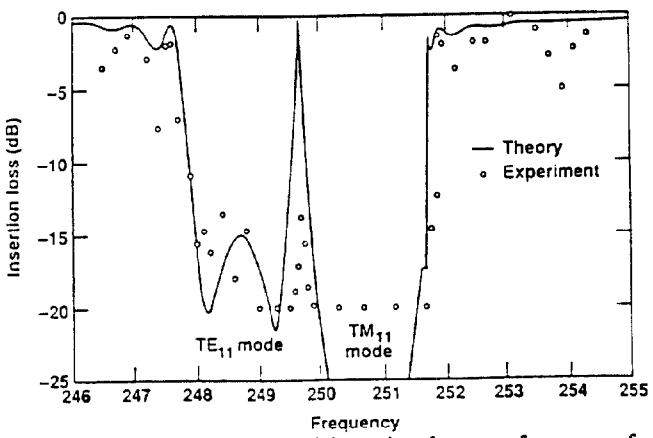

Fig.3. Calculated and measured insertion loss vs. frequency for a 300 ripple, 25 μm amplitude, 7-mm-diam Bragg section.

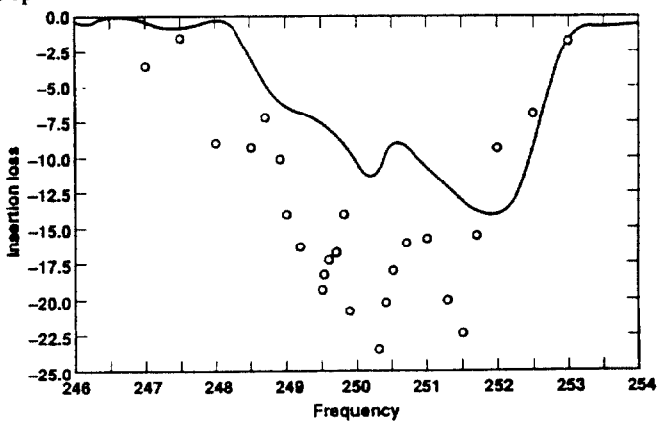

Fig.4. Calculated and measured insertion loss vs. frequency for a 150 ripple, 25 μm amplitude, 7-mm-diam Bragg section.

III. Diffraction Tank Design and Performance

A sketch of the CARM diffraction tank is shown in Fig. 5. Microwave energy is generated in the CARM device collinear with the electron beam; the latter is deflected into the beam dump wall by means of 900 Gauss permanent magnet. The microwave beam is radiated from a 28-mm-diam aperture at the upstream end of the beam dump. The $1/e^2$ contour of the quasioptical beam at 250 GHz will clear the end of the beam-dump; the K_a band signal propagates as in overmoded waveguide. Higher modes may exist and must be taken into account in interpreting the data. The 250 GHz diagnostic consists of two WR4 waveguide stubs, with or without gain horns, at the back flange. A vacuum seal is achieved by means of a thin mica washer and O-ring arrangement, clamped between the WR4 flanges. Both stubs are rotatable to allow a polarization check. Additional attenuation is introduced by a collimating aperture that slides into the tank from one end. K_a band power is monitored by a WR28 waveguide stub that is positioned at the -10 dB point of the main TE_{11} lobe at 25 GHz. An additional, uncalibrated monitoring port is drilled directly into the beam dump wall, and is connected to a standard WR28 waveguide, vacuum window.

Prior to fabrication of the actual diffraction tank, we simulated the configuration on an optical bench, using the same transmitter-receiver combination shown in Fig. 2. Using a simple, free-space transmission model, with standard expressions for antenna gain, we were able to predict the measured, 250 GHz transmission loss within 2-5 dB, even for the case where the collimating aperture was inserted (Figs. 6,7). On the actual tank, the overall attenuation was measured by direct substitution, yielding 32-38 dB at K_a band and 30-36 dB at 246-254 GHz, depending on the collimator aperture. Agreement with the theory was very poor for the off-axis attenuation at K_a band, and within 10 dB at 250 GHz. The greater, measured values at 250 GHz agree more closely with the calculated attenuation for the TE_{12} mode, and this may indicate substantial mode conversion, e.g., at the wall discontinuity near the beginning of the beam dump.

IV. Conclusion

Insertion loss measurements at 250 GHz on two, 300 ripple, 25 μm amplitude, 7 mm diam, Bragg sections gave excellent agreement with the theory. Similar measurements with sections of half that length gave good agreement in terms of the frequency range but yielded an insertion loss that was some 10 dB greater than the model predicted. We believe this may be due to poorer mode separation and stronger mode coupling for the shorter section. Attenuation measurements at 250 GHz made on an optical-bench replica of the CARM diffraction tank gave agreement with modeling predictions within 2-5 dB. Measured loss on the actual tank was 10 dB greater than predicted, probably due to mode conversion at the beam dump discontinuity.

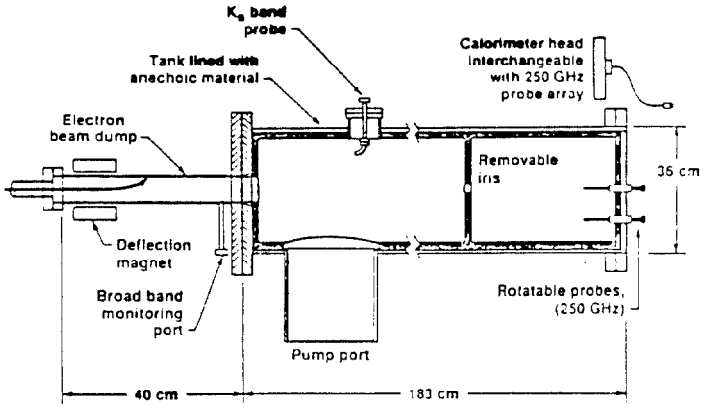

Fig.5. Sketch of CARM microwave diffraction tank.

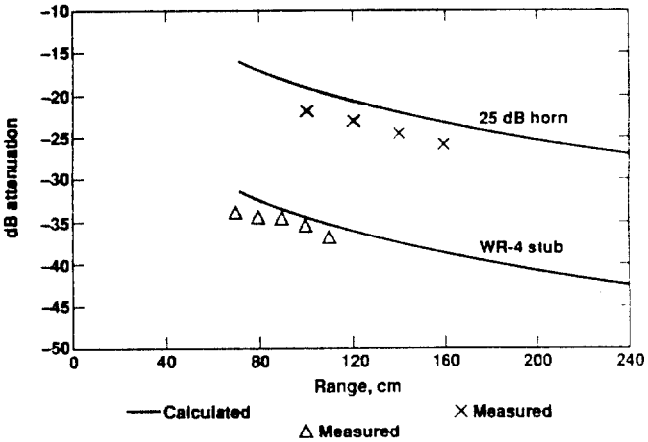

Fig.6. Calculated and measured attenuation vs. range, for simulated diffraction tank geometry, without collimating aperture.

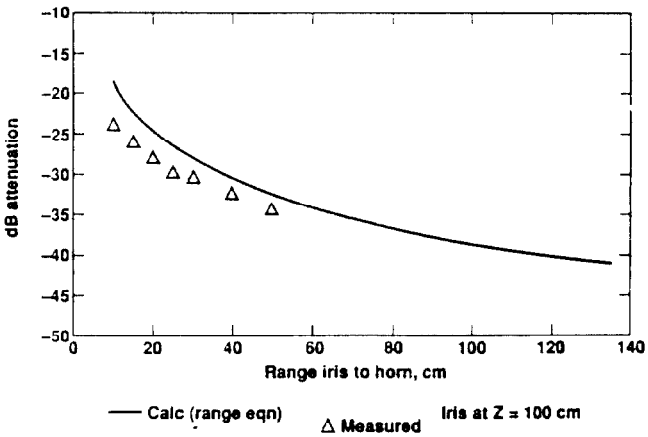

Fig.7. Calculated and measured attenuation vs. range from collimating aperture to receiver, simulated diffraction tank geometry.

V. References

[1] V. L. Bratman, G. G. Denisov, N.S. Ginzburg, and M. I. Petelin, "FEL's with Bragg Reflection Resonators: Cyclotron Autoresonance Masers Versus Ubitrons," *IEEE J. Quantum Electronics QE-19*, p. 282, 1983.

[2] B. Kulke, M. Caplan, D. Bubp, T. Houck, D. Rogers, D. Trimble, R. VanMaren, G. Westenskow, D. B. McDermott, N. C. Luhmann, Jr., and B. Danly, "Test Results from the LLNL 250 GHz CARM Experiment," this Proceedings.